J Appl Electrochem (2012) 42:979–987
DOI 10.1007/s10800-012-0466-5

ORIGINAL PAPER

Multiwalled carbon nanotube-4-*tert*-butyl calix[6]arene composite electrochemical sensor for clenbuterol hydrochloride determination by means of differential pulse adsorptive stripping voltammetry

Reena R. Gaichore · Ashwini K. Srivastava

Received: 19 April 2012 / Accepted: 22 July 2012 / Published online: 9 August 2012

Abstract The electrochemical behavior of clenbuterol hydrochloride (CLB) was studied at a multiwalled carbon nanotube-4-*tert*-butyl calix[6]arene composite chemically modified electrode by means of cyclic voltammetry, electron impedance spectroscopy, and differential pulse adsorptive stripping voltammetry. Surface characterization of the electrode was carried out by means of SEM. The results revealed that 4-*tert*-butyl calix[6]arene along with multiwalled carbon nanotubes demonstrated a high sensitivity for determination of CLB. Employing differential pulse adsorptive stripping voltammetry allowed a linear response over the concentration range of 1.99×10^{-8}–4.76×10^{-5} M with a detection limit of 1.38×10^{-9} M for CLB. The described method has been applied for the estimation of CLB in biological fluids such as urine and serum.

Keywords Electrochemical sensor · Clenbuterol hydrochloride · Voltammetry · Biological fluids

1 Introduction

Clenbuterol hydrochloride (CLB), a β-agonist cardiovascular drug, is known for stimulating β-receptors reducing stress symptoms and asthma and has been extensively used in the treatment of human depression and pulmonary disease [1]. The high levels of this drug in the human body may lead to muscular tremor, heart throb, glaucoma, prostatitis, and even death in aged people [2]. Thus, the determination of CLB in human body fluids is of immense importance.

Different techniques have been described for the determination of CLB, including chromatography [3–7], of which some are devoted to studying the β-agonists-macrocyclic interactions [8–13], capillary electrophoresis [14–17] and spectrophotometry [18, 19]. However, some of these methods are associated with several shortcomings including high cost, long analysis time, and short column lifetime. Capillary electrophoresis is also recognized to be a powerful and versatile technique for chiral drugs for its speed, efficiency, and reproducibility. Despite these inherent characteristics, one drawback is the lack of sensitivity owing to the much reduced detection path and very small volumes of the sample injected, while in spectrophotometric analysis, direct analysis lacks sensitivity. The application of potentiometric detection is known to strongly reduce the matrix interference effect for UV-absorbing compounds which are eluted early from HPLC columns [20–22]. It was also applied for the discrimination of certain β-adrenergic drugs extended by the use of supramolecular systems inducing host–guest interactions [9].

The presence of an electroactive aromatic group in CLB can lead to its electrochemical analysis, which is cheap and convenient. Electrochemical techniques, by means of stripping voltammetry, are particularly suited for these applications [23–28]. Carbon paste electrodes (CPEs) exhibit unique properties such as low background currents, a favorable anodic potential range, extraction capabilities, and an easily renewable electrode surface. Electrochemical methods using porous carbon, nafion-modified carbon paste, and multiwalled carbon nanotube–nafion nanocomposite electrode have also been used for the detection of CLB in pharmaceutical and biological matrices [29, 30].

R. R. Gaichore · A. K. Srivastava (✉)
Department of Chemistry, University of Mumbai, Vidyanagari, Santacruz (East), Mumbai 400 098, India
e-mail: aksrivastava@chem.mu.ac.in; akschbu@yahoo.com

Carbon nanotubes (CNTs), especially multiwalled carbon nanotubes (MWCNTs), are long known to be excellent catalysts due to their smooth, straight, one dimensional channel at the center which can hold atoms or molecules [30]. Due to these interesting aspects, they have been widely used in the construction of sensors and nanoscale electronic devices. On the other hand, macrocyclic ligands have attracted much attention in recent times due to their excellent capability for molecular recognition. The strong affinity of calixarenes can be explained on the basis of their large cavities and ionisable carboxylic acid groups insuring electrostatic interactions [31, 32]. We have recently reported successful electrochemical sensors based on macrocyclic ligands [33, 34].

The present work demonstrates an application of multiwalled carbon nanotube-4-*tert*-butyl calix[6]arene composite chemically modified electrode (C[6]-CNT-CME) to postulate a redox mechanism for CLB and to detect it to trace levels by differential pulse adsorptive stripping voltammetry (DPAdSV). In the present approach, the advantages of 4-*tert*-butyl calix[6]arene and the high electrocatalytic activity of MWCNTs are combined to exhibit their synergistic effect toward the redox behavior of CLB. The experimental conditions are optimized and performance features such as reproducibility and stability are evaluated. The developed method has been applied for biological samples viz, human serum and urine.

2 Experimental

2.1 Chemicals and instrumentation

All chemicals were of AR Grade and were used as received without any further purification. CLB was purchased from Sigma. MWCNTs (dimensions: OD 60–100 nm, ID = 5–10 nm, length = 0.5–50 μm, (95+ %)) were obtained from Aldrich (USA). Graphite powder was purchased from S. D. Fine (India). Paraffin oil was purchased from Fluka (USA). 4-*tert*-butyl calix[6]arene was purchased from Aldrich and all other chemicals including glucose, starch, lactose, dextrose, oxalic acid, urea, tartaric acid, and trisodium citrate were of (A.R.) grade and used without further purification. The solutions were prepared using double distilled water of specific conductivity 0.3–0.8 μS.

All voltammetric measurements were performed on an Eco-Chemie, Electrochemical Work Station, Model Autolab PGSTAT 30 (The Netherlands) having the GPES software (Version 4.9.005). All pH measurements were performed using ELICO Li 120 pH meter. An Ag/AgCl electrode and a platinum counter electrode were used as reference and counter electrodes, respectively. All potentials were measured with respect to Ag/AgCl (aq) (3 M KCl) as the reference electrode. A plain carbon paste electrode (PCPE), a 4-*tert*-butyl calix[6]arene chemically modified electrode (C[6]-CME), a MWCNT-modified electrode (CNT-CME), and a 4-*tert*-butyl calix[6]arene-MWCNT-modified electrode (C[6]-CNT-CME) were used as working electrodes. The UV–Vis spectrophotometer (Shimadzu, Japan) was used for validating the method. The scanning electron microscope employed for surface characterization of the electrodes was a FEI Quanta-200 model with an operating voltage of 20 kV.

2.2 Fabrication of the electrodes

The PCPE was prepared using slurry composed of 70:30 graphite: paraffin oil using a mortar and pestle, which was then allowed to homogenize for 48 h. The C[6]-CME was prepared in the same manner as the PCPE, but by dispersing a weighed quantity of 4-*tert*-butyl calix[6]arene in acetone and adding appropriate amount of graphite powder to form the modified graphite powder. The slurry was stirred to evaporate all the acetone. A required quantity of paraffin oil was added as a binder. For the modified electrode, C[6]-CME, the ratio was 65 % of graphite:5 % of 4-*tert*-butyl calix[6]arene:30 % of paraffin oil.

For the preparation of C[6]-CNT-CME, the CNTs were pre-treated. During this pre-treatment, 0.05 g of carbon nanotubes were dispersed into 60 mL of 2.2 M HNO_3 for 20 h at room temperature with the aid of ultrasonic agitation, then washed with distilled water to neutrality, and dried in the oven at 37 °C [35]. Modification of the electrode was done by mixing the appropriate amount of CNTs with 4-*tert*-butyl calix[6]arene, and dispersing the mixture in acetone and the required amount of graphite powder. The ratio of these components in the modified electrode was 60 % of graphite:5 % of 4-*tert*-butyl calix[6]arene:5 % of MWCNT:30 % of paraffin oil. The CNT-CME was also prepared in a similar fashion, but in the absence of 4-*tert*-butyl calix[6]arene, in the ratio 65:5:30. The paste thus obtained was filled in a 2-ml glass syringe. A copper wire inserted in the paste was used to establish electrical contact. Smooth and fresh electrode surfaces were obtained by squeezing out 0.5 mm of paste from the syringe, scraping off the excess, and polishing it against butter paper until the surface had a shiny appearance. The electrodes could be used for a period of 6 months without any degradation in electrochemical properties.

2.3 General analytical procedure

For stripping voltammetric analysis of CLB, appropriate quantities of the analyte solution were placed in a 25-mL volumetric flask and then diluted to the mark with Britton-Robinson (BR) buffer, pH 1.5. The solution was then

transferred into the micro-electrochemical cell when the measurements were carried out. A magnetic stirrer (Expo Hi-Tech, India) with a stirring bar was used to provide the convective transport of the analyte during its accumulation onto the carbon paste electrode surface. An accumulation potential of −0.20 V was applied to the C[6]-CNT-CME for an accumulation duration of 180 s while the solution was stirred at 300 rpm with the magnetic stirrer. The test solutions were purged with nitrogen for 5 min initially. At the end of the accumulation period, the stirring was stopped and a 10 s rest period was allowed for the solution to become quiescent before recording the cyclic voltammetry (CV) and DPAdSV. CVs were carried out at the optimized conditions for CLB at a scan rate of 50 mV s^{-1}. The DPAdSVs were recorded by scanning the potential toward the positive direction from +0.70 to +1.50 V by means of a scan rate of 10 mV s^{-1} and modulation amplitude of 50 mV. Recovery tests were performed by spiking standard solutions of CLB into biological fluids including urine and blood serum samples from healthy volunteers. Human blood serum samples were obtained from a local pathology clinic and stored under refrigeration.

3 Results and discussion

3.1 Cyclic voltammetry

Cyclic voltammetry (CV) was used to establish the potential window in BR buffer medium, which was found to be 0.00 to +1.30 V. In this potential range, the influence of the presence of modifier in the carbon paste matrix of the working electrode was studied. Figure 1 gives the comparison of the CVs at PCPE (A), C[6]-CME (B), CNT-CME (C), and C[6]-CNT-CME (D). The resulting peak potential for CLB at

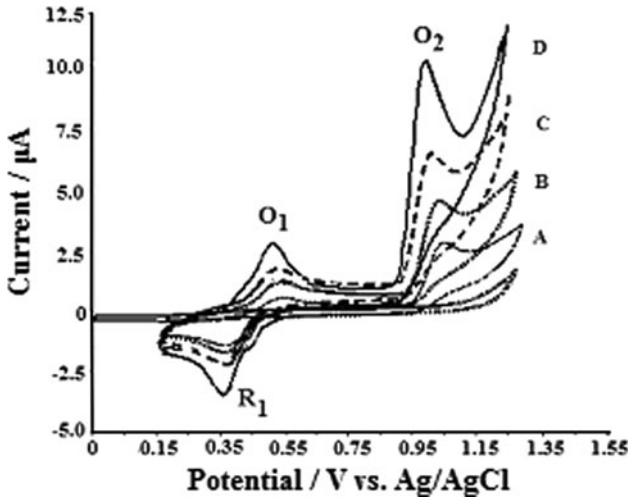

Fig. 1 CVs for 2.44 × 10^{-4} M CLB at PCPE (*A*), C[6]-CME (*B*), CNT-CME (*C*), and C[6]-CNT-CME (*D*) in B. R. buffer pH 1.5 at 50 mV s^{-1}

PCPE was +1.01 V whereas the peak potential obtained at C[6]-CNT-CME was +0.95 V. Thus, it could be concluded that the electro-oxidation of CLB became facile at the C[6]-CNT-CME surface. Furthermore, the peak currents at both the CMEs are much larger than PCPE. The redox peak currents are nearly double at C[6]-CME in comparison to PCPE. The interaction of CLB with 4-*tert*-butyl calix[6]arene is relevant to the amino-calix[n]arene interactions reported elsewhere [31, 32]. The specific interaction of 4-*tert*-butyl calix[6]arene and the guest molecule, CLB, can be explained on the basis of the arrangement of the functional groups of 4-*tert*-butyl calix[6]arene toward the –NH groups of CLB and the favorable length of the alkyl chains. On the other hand, the important parameters for CLB are its hydrophobicity, ionic property, steric environment around the –NH groups, and the number of hydrogen bonds for the most effective co-ordination. This strong binding of 4-*tert*-butyl calix[6]arene is effective in recognizing CLB, and hence is expected to be a novel recognition tool for CLB, explaining the twofold increment in current for CLB at C[6]-CME over PCPE. As observed from Fig. 1, CLB exhibited an irreversible anodic peak at +0.95 V at C[6]-CNT-CME which is found to give a cathodic peak at +0.36 V on adsorption. This cathodic peak gives a subsequent anodic peak at +0.40 V, thus forming a quasi-reversible couple. A similar electrochemical behavior has been previously reported [28, 30]. Further, the current intensities for these peaks at C[6]-CNT-CME were observed to increase by another twofold which can be attributed to the synergistic effect of both MWCNTs and 4-*tert*-butyl calix[6]arene. The MWCNTs with closed topology and much larger surface area exhibited a strong adsorptive ability toward CLB, thus enhancing the surface concentration.

3.1.1 Effect of pH

The effect of pH was evaluated for CLB in the pH range of 1.5–12.0. It was observed that the solution of pH 1.5 gave a well-defined peak with the highest current and thus was selected for further study. Also, it was observed that there was no shift in the peak potential of the irreversible peak at +0.95 V with increase in pH inferring that there is no proton involvement in the reaction. Further, in order to elucidate the reaction mechanism and rate determining step in the electrocatalytic irreversible oxidation of CLB, CVs were obtained at different scan rates, *v*, at C[6]-CNT-CME (Fig. 2). For an irreversible oxidation of CLB at +0.95 V, α is presumed to be 0.5 [36], then by substituting the value of "α" in the equation

$$E_p - E_p/2 = 47.7/\alpha n_a \text{ at } 25^{\circ}\text{C} \quad (1)$$

the "n_a" value is found to be "1" showing one electron involvement in the reaction. The current of this peak drops

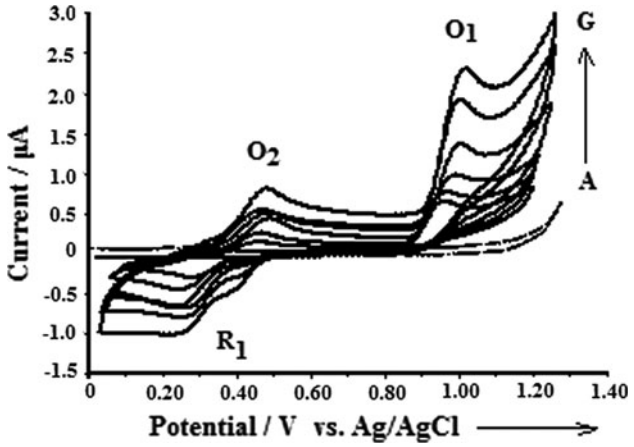

Fig. 2 CVs obtained at different scan rates, v, at C[6]-CNT-CME for 3.84×10^{-5} M CLB in B. R. Buffer pH 1.5; (*A*) 25, (*B*) 50, (*C*) 100, (*D*) 150, (*E*) 200, (*F*) 250, and (G) 500 mV s^{-1}

sharply in the next scan, suggesting an adsorbed process on the electrode. Further, in the return scan, CLB shows a peak at +0.36 V and in the second cycle, the CV shows two well-defined anodic peaks and one cathodic peak at O_1 (+0.95 V), O_2 (+0.40 V), and R_1 (+0.36 V), respectively. Thus, CLB was irreversibly oxidized at a high potential with a subsequent chemical reaction, giving rise to a product which exhibits the quasi-reversible couple.

To assess the reversibility of the reaction, a newly renewed electrode was scanned between 0 and +0.60 V, a potential lower than the oxidation potential of CLB. However, the reduction peak (R_1) on the reverse scan and the subsequent reoxidation peak (O_2) on the forward scan were found to be absent, suggesting the quasi-reversible couple due to the oxidation product formed at O_1. The quasi-reversible couple is considered to be the result of the sp^2 hybridization occurring at the nitrogen atoms forming a dimer of CLB with an azo-bond [28].

The pH study for the quasi-reversible couple showed that with the increase in pH, there was a shift in peak potential of O_2 toward less positive values indicating the proton transfer participation in the reaction. The slope of E_p versus pH (Fig. 3) was found to be 50.38 mV for CLB from which the m/n value of 1 was estimated. From the cyclic voltammogram, a difference in anodic and cathodic potentials (ΔE_p) of 40 mV is observed for the quasi-reversible couple at a scan rate of 50 mV s^{-1} with a formal potential, $E^{0\prime} = (E_{pa} + E_{pc})/2 = -160$ mV, indicating a two electron transfer process [37]. Considering the m/n value of 1, involvement of an equal number of electrons and protons ($2e^-$ and $2H^{+)}$ is ascertained. The relationship between peak currents of both the anodic peaks and the scan rates in BR buffer pH 1.5 was observed by means of CV. A plot of peak current of the anodic peak at O_1 versus square-root of the scan rate is linear, indicating the process to be diffusion controlled. The regression equation for this relationship is as follows: $I_p = 4.178v^{1/2} + 0.705$ ($R = 0.992$) (Fig. 4a). However, the peak current for the anodic peak, O_2, is proportional to the scan rate, revealing the process to be adsorption controlled (Fig. 4b). Therefore, the peak $O_1$was considered for further study by DPV and DPAdSV.

3.2 Effect of varying percentage of modifiers on the oxidation peak of CLB

The effect of the amount of 4-*tert*-butyl calix[6]arene as a modifier in the carbon paste was first studied by varying its composition in the range of 1–10 % with respect to graphite by DPV. It was then observed that the oxidation peak current of CLB increased with an increase in the percentage of 4-*tert*-butyl calix[6]arene up to 5 %, beyond which the peak current leveled off. Similarly, on varying the amount of MWCNTs as a modifier in the carbon paste in the range of 1–10 %, it was observed that the oxidation

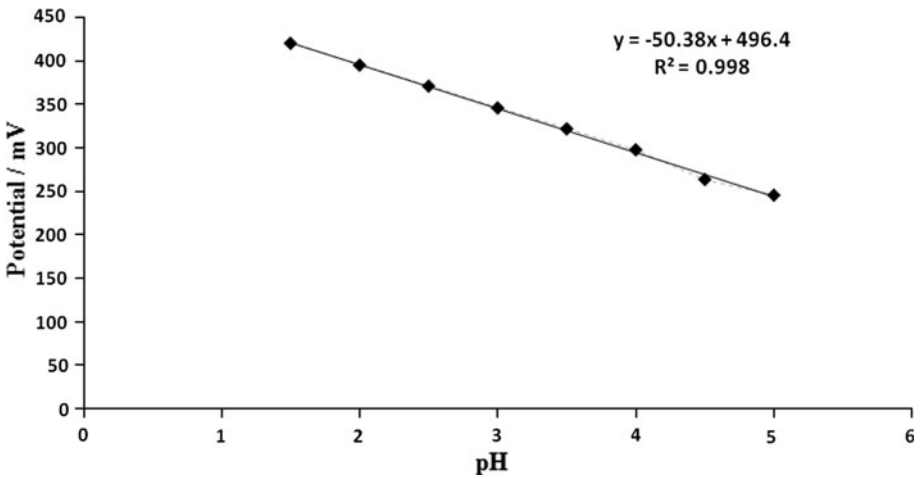

Fig. 3 Plot of E_p versus pH for the peak O_2 on C[6]-CNT-CME. CLB concentration "c" = 3.85×10^{-5} M, accumulation potential = −0.2 V, accumulation time = 180 s

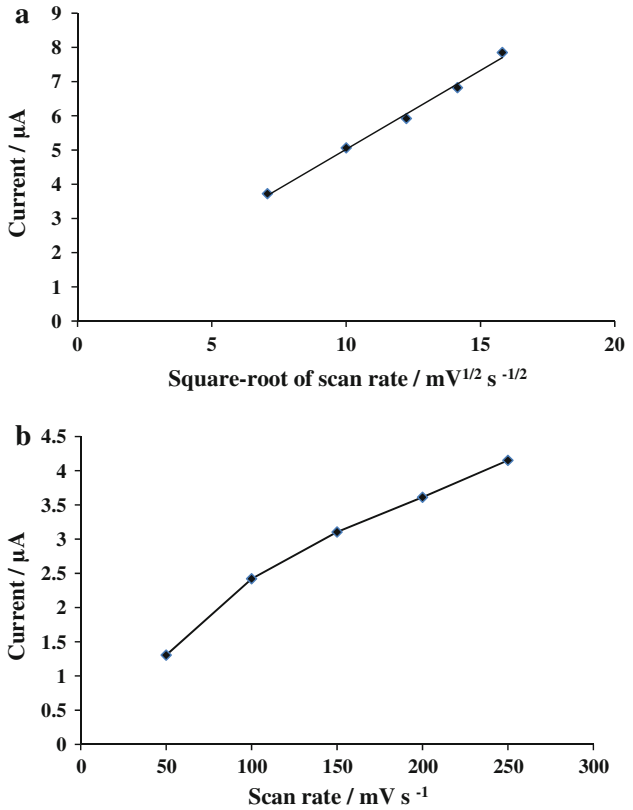

Fig. 4 **a** Plot of I_p versus $v^{1/2}$ for the peak O_1 on C[6]-CNT-CME in BR buffer pH 1.5 containing 3.85×10^{-5} M CLB. **b** Plot of I_p versus v for peak O_2 on C[6]-CNT-CME in BR buffer pH 1.5 containing 3.85×10^{-5} M CLB

peak current of CLB increased with an increase in the percentage of MWCNTs up to 5 %, beyond which saturation in the anodic peak current occurs. As a result, 5 % of 4-*tert*-butyl calix[6]arene and 5 % of MWCNTs were selected as the optimum amounts for the preparation of the C[6]-CNT-CME. The results using different electrodes are summarized in Fig. 5.

3.3 Scanning electron microscopy (SEM) characterization and electrochemical impedance study (EIS) of CLB at the modified electrodes

Scanning electron microscopy (SEM) was employed for the characterization of the modified electrodes. Figure 6 displays the morphologies of PCPE (a), C[6]-CME (b), and C[6]-CNT-CME (c). As observed from Fig. 6c, 4-*tert*-butyl calix[6]arene distributed on the surface of graphite particles offers a highly accessible surface area for host–guest interaction, and the spaghetti-like fragments of carbon nanotubes provide smooth, straight, one dimensional channels at the center which can hold atoms or molecules with a much larger surface area exhibiting strong adsorptive abilities toward CLB. Thus, along with the host–guest

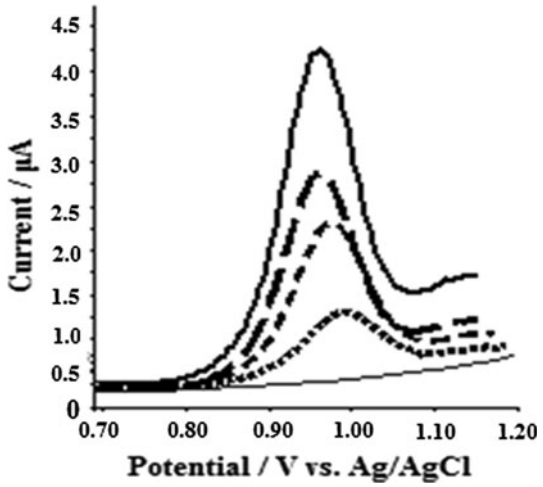

Fig. 5 DPAdSVs for 5.02×10^{-6} M CLB at PCPE (*thin dotted line*), C[6]-CME (*thick dotted line*), CNT-CME (*dashed line*), and C[6]-CNT-CME (*thin line*) in BR buffer pH 1.5 at scan rate, 10 mV s^{-1}; pulse height, 50 mV; $E_{acc} = -0.2$ V; and $t_{acc} = 180$ s

interactions, the nanometer dimension of the CNTs, their electronic structure, and the topological defects present on their surface are responsible for accelerating the electron transfer between CLB and the electrode surface [38]. This leads to an improvement in their surface concentration leading to increased response of CLB in terms of peak current at its surface than PCPE, hence allowing a greater catalytic effect.

An EIS study was performed to evaluate the influence of surface kinetics of PCPE (A), C[6]-CME (B), CNT-CME (C), and C[6]-CNT-CME (D) in BR. buffer pH 1.5 containing 1.08×10^{-4} M CLB (Fig. 7) in the frequency range 10^{-2}–10^{6} Hz. The EIS data obtained were further analyzed to examine the exact fitting equivalent circuit. As an evidence of the plot of *Z*-real versus *Z*-imaginary, a mixed kinetic and diffusion control type of circuit was obtained for all the three electrodes. Similar type of Nyquist plots were obtained for PCPE (A), C[6]-CME (B), CNT-CME (C), and C[6]-CNT-CME (D). In this figure, the semicircle part corresponds to the charge transfer-limited process. The corresponding circuit is presented in the inset figure, which is made up of the electrolyte solution resistance (R_Ω) in series with the parallel circuit of Faradaic Impedance (Z_f) and double layer capacitance (C_{dl}). Z_f is composed of charge-transfer resistance (R_{ct}) and Warburg impedance (Z_w). From the plot of *Z*-real vs. *Z*-imaginary, it can be seen that the R_{ct} is relatively less and depressant for C[6]-CNT-CME in comparison to PCPE, and this is a result of a mixed kinetic diffusion controlled type of circuit, which is indicated by a decrease in diameter of the semicircle curve (Fig. 7). Thus, the above diagnosis of the observed impedance spectra revealed that the kinetically facile

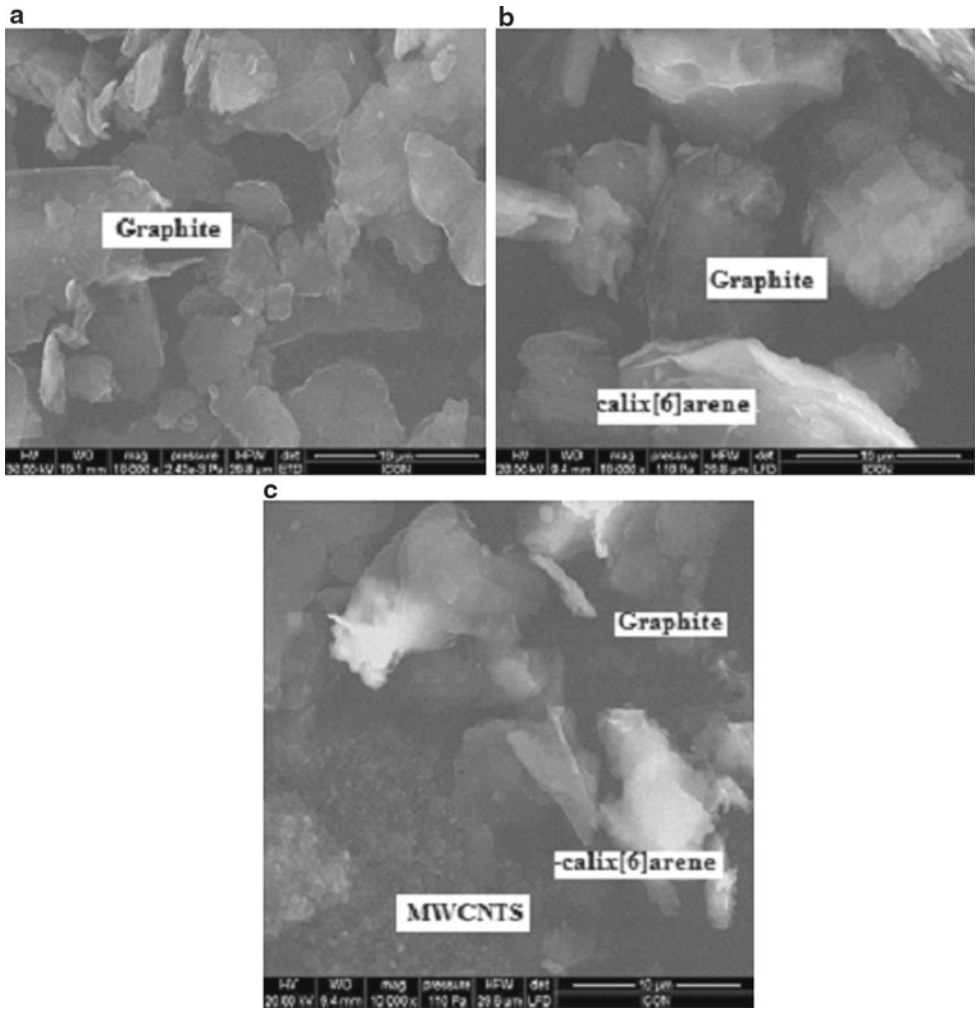

Fig. 6 SEM images of the typical morphologies of PCPE (**a**), CME-6 (**b**), and C[6]-CNT-CME (**c**)

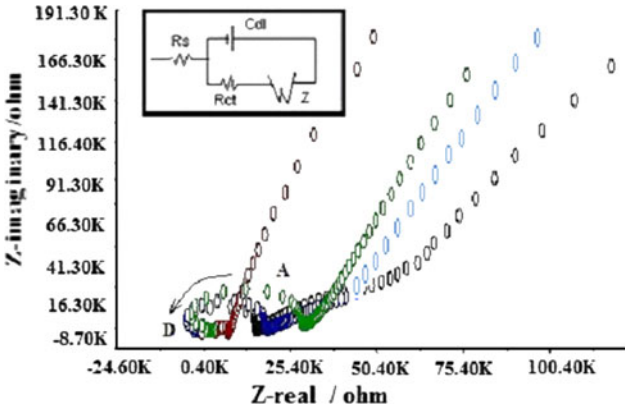

Fig. 7 Electrochemical impedance spectra for 5.88×10^{-5} M CLB on PCPE (*A*), CME-6 (*B*), CNT-CME (*C*), and C[6] CNT-CME (*D*) in BR buffer pH 1.5 at the frequency range of 10^{-2}–10^{6} Hz; the *inset* figure presents the mixed kinetic diffusion control type of circuit

nature of CLB at the modified electrodes is in the order of PCPE < C[6]-CME < CNT-CME < C[6]-CNT-CME.

3.4 Differential pulse adsorptive stripping voltammetric determination of CLB

For DPAdSV, the effect of accumulation time (t_{acc}) and accumulation potential (E_{acc}) was studied at C[6]-CNT-CME. By maintaining a constant t_{acc} as 120 s, E_{acc} was determined by employing a potential window of −0.20 to +1.30 V. Figure 8a presents the effect of different accumulation potentials toward the electrochemical behavior of CLB at C[6]-CNT-CME. It was observed that the peak current reached its maximum at an E_{acc} of −0.2 V. Likewise, it was observed that an increase in the accumulation time improved the sensitivity of determination. Hence, the effect of variation of t_{acc} was studied over a period of 10–300 s, keeping $E_{acc} = -0.2$ V constant at a concentration of 2.91×10^{-5} M CLB. It was observed that from 10 to 180 s, there was a linear increase in the peak current of CLB (Fig. 8b). Beyond this range, the current began to level off. This observation implied that surface saturation occurred at higher accumulation times. Thus, t_{acc} of 180 s

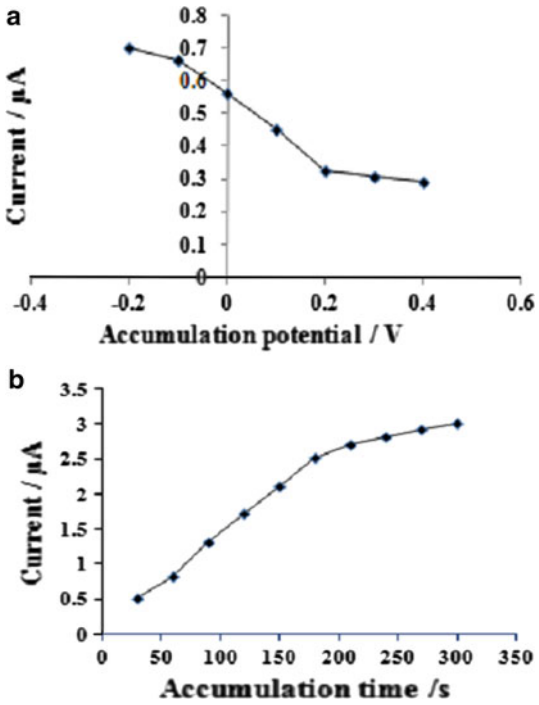

Fig. 8 **a** Effect of different accumulation potentials (E_{acc}) for 1.96×10^{-5} M CLB at C[6]-CNT-CME in BR buffer pH 1.5. **b** Effect of different accumulation times (t_{acc}) for 2.91×10^{-5} M CLB at C[6]-CNT-CME in BR buffer pH 1.5

was selected as the optimum time where the analyte could be determined with good sensitivity.

From these experiments, it could be observed that the best results for both peak current and peak potential were obtained at C[6]-CNT-CME. An overall significant four-fold increment in peak current was observed at the modified electrode, C[6]-CNT-CME, for an accumulation potential of −0.2 V and an accumulation time of 180 s. The linear response over the concentration range of 1.99×10^{-8} to 4.76×10^{-5} M and a detection limit of 1.38×10^{-9} M (three times the signal-to-noise ratio, $S/N = 3$) ($r = 0.998$) is observed for CLB at the modified electrode with a linear regression curve as I_p (μA) = 3.210 C (10^{-6} M) + 29.47 by means of DPAdSV. A relative standard deviation of 1.35 % was observed for ten successive measurements of 1.96×10^{-6} M, which suggested good reproducibility for CLB determination. The intra-day and inter-day RSD% were found to be 1.35 and 1.41 %, respectively.

Table 2 Recovery for CLB estimation in biological fluids by the proposed method

Biological fluid	I	II	III	IV
Human serum				
	9.56×10^{-7}	9.43×10^{-7}	98.64	
	1.59×10^{-6}	2.51×10^{-6}	99.09	99.25
	3.19×10^{-6}	5.65×10^{-6}	99.12	
	3.83×10^{-6}	3.84×10^{-6}	100.18	
Human urine				
	1.59×10^{-6}	1.56×10^{-6}	98.11	
	3.19×10^{-6}	4.74×10^{-6}	99.78	99.39
	3.83×10^{-6}	8.60×10^{-6}	100.35	
	4.78×10^{-6}	1.33×10^{-5}	99.25	

I Concentration added (M); *II* Concentration found (M); *III* Recovery (%); *IV* Average recovery (%)

3.5 Interference studies

The effects of common excipients and other additives were tested for their possible interferences in the assay of CLB. It was observed that the other concomitants such as glucose, starch, lactose, dextrose, oxalic acid, urea, tartaric acid, and trisodium citrate did not interfere in the determination of CLB at the levels normally found in dosage forms (up to 200 fold). These results suggested that the determination of CLB in biological fluids at C[6]-CNT-CME was not significantly affected by the most common interfering species.

3.6 Determination of CLB in biological fluids

For analytical applications, the determinations of the amount of CLB in biological fluids have been carried out by the standard addition method. The proposed method was validated by UV–Vis spectrophotometry [19] and the results are given in Table 1. It is found that the amount of CLB obtained by the proposed method agreed well with the amount obtained by the standard methods.

For further evaluation of the validity of the proposed method, recovery tests for CLB in human urine and serum samples were performed. Aliquots of human serum samples were fortified with different concentrations of CLB and diluted to 10 mL with BR buffer pH 1.5 to obtain concentrations of 0.95–3.83×10^{-6} M in the serum. Then,

Table 1 Validation of the proposed method for CLB determination in biological fluids

Biological fluid	I	II	III [19]
Human serum	9.56×10^{-7}	$9.48 \times 10^{-7} \pm 0.06$ ($n = 5$)	$8.97 \times 10^{-7} \pm 0.04$ ($n = 5$)
Human urine	1.59×10^{-6}	$1.58 \times 10^{-6} \pm 0.04$ ($n = 5$)	$1.53 \times 10^{-6} \pm 0.03$ ($n = 5$)

I Concentration added (M); *II* Concentration found by proposed method (M); *III* Concentration found by UV spectrophotometric method (M)

Table 3 Comparison of the proposed method with other voltammetric methods

S. no.	Sensor	Technique	Linear range (M)	Detection limit	References
1.	BDD	PAD	5.00×10^{-7}–5.00×10^{-5}	–	[2]
2.	PD-BDD	–	3.40×10^{-6}–5.00×10^{-4}	8.50×10^{-7}	[25]
3.	GCE	CV, LSV, SWSV	3.00×10^{-7}–1.00×10^{-5}	5.10×10^{-8}	[26]
4.	SBME	DPV	–	–	[27]
5.	NAF-AuE	DPV	8.00×10^{-7}–1.00×10^{-5}	1.00×10^{-7}	[28]
6.	NAF-CPE	DPV	–	1.02×10^{-9}	[29]
7.	CNT-NAF-E	DPA	1.00×10^{-9}–1.00×10^{-6}	5.00×10^{-10}	[30]
8.	C[6]-CNT-CME	DPAdSV	1.52×10^{-8}–4.76×10^{-5}	1.39×10^{-9}	Present work

BDD Boron-doped diamond thin film; *PD* Pyrrole-DNA modified; *GCE* Glassy carbon electrode; *SBME* Solid binding matrix/molecularly imprinted polymer-based sensor; *NAFAuE* Nafion-Au colloids-modified GCE; *NAF-CPE* Nafion-modified CPE; *CNT-NAF-E* MWCNT-Nafion-modified GCE; *PAD* Pulsed amperometry; *DPA* Differential pulse amperometry

the spiked serum samples were directly analyzed according to the proposed voltammetric procedure. Similarly, urine samples were spiked with different aliquots of CLB using BR buffer to obtain the concentrations of 1.59–4.78×10^{-6} M in the urine. Then, the solution was directly analyzed according to the proposed voltammetric procedure. Based on these results, recovery results were not affected significantly (Table 2) and, consequently, the described method was accurate for the assay of CLB in complex matrices.

A comparison between the analytical performance of the present method and some previous literature methods for the determination of CLB is given in Table 3. The detection limit obtained by the proposed method is in congruence with the other reported methods. Thus, the proposed C[6]-CNT-CME has many advantages such as a good linear working range, a comparable detection limit, biological fluid analysis, and simplicity in preparation as well as surface renewability in addition to the novel synergistic approach using a macrocycle, 4-*tert*-butyl calix[6]arene, and MWCNTs.

4 Conclusions

The results obtained in the present work demonstrate the synergism of 4-*tert*-butyl-calix[6]arene and MWCNTs toward the stripping voltammetric determination of CLB exhibiting shift of peak potentials toward less negative potentials. Additionally, the oxidation peak current was observed to remarkably increase at C[6]-CNT-CME surface. Moreover, the proposed method was very sensitive, free of common interferences, and had a sub-micromolar detection limit. This method can be employed for CLB detection in urine and blood serum samples. Thus, the proposed method can be recommended for trace level detection of CLB in clinical and quality control laboratories.

References

1. Peng K, Tang X, Xiang S (2006) Zhongguo Weisheng Jianyan Zazhi 16:307
2. Karuwen C, Mantim T, Chaisuwan P, Wilairat P, Grudpan K, Jittangprasert P, Einaga Y, Chailapakul O, Suntornsuk L, Anurukvorakun O, Nacapricha D (2006) Sensors 6:1837
3. Zheng H, Deng L–G, Lu X, Zhao S-C, Guo C-Y, Mao J-S, Wang Y-T, Yang G-S, Aboul-Enein H-Y (2010) Chromatographia 72:79
4. Vonaparti A, Lyris E, Angelis YS, Panderi I, Koupparis M, Tsantili- Kakoulidou A, Peters RJB, Nielen MWF, Georgakopoulos C (2010) Rapid Commun Mass Spectrom 24:1595
5. Lu M, Zhang L, Li X, Lu Q, Chen G, Cai Z (2010) Talanta 81:1655
6. Corcia DD, Morra V, Pazzi M, Vincenti M (2010) Biomed Chromatogr 24:358
7. Peters RJB, Oosterink JE, Stolker AAM, Georgakopoulos C, Nielen MWF (2010) Anal Bioanal Chem 396:2583
8. Bazylak G, Nagels LJ (2003) J Pharm Biomed Anal 32:887
9. Bazylak G, Nagels LJ (2003) Farmaco 58:591
10. Bazylak G, Nagels LJ, Monge ME (2003) Chromatographia 57:757
11. Bazylak G, Nagels LJ (2002) Curr Med Chem 9:1547
12. Nagels LJ, Bazylak G, Zielinska D (2003) Electroanalysis 15:533
13. Koide T, Ueno K (2000) J Chromatogr A 893:177
14. Jiao F, Chen X, Hu Y, Wang Z (2008) J Iran Chem Soc 5:553
15. Bazylak G, Monge ME, Everaert J, Nagels LJ (2009) J Sep Sci 32:135
16. Gausepohl C, Blaschke G (1998) J Chromatogr B Biomed Sci Appl 713:443
17. Na Na, Hu Y, Ouyang J, Baeyens Willy RG, Delanghe JR, Taes Youri EC, Xie M, Chen H, Yang Y (2006) Talanta 69:866
18. Lopez-Erroz C, Vinas P, Cerdan FJ, Hernandez-Cordoba M (2000) Talanta 53:47
19. Biosca YM, Baeza Baeza JJ, Ramis-Ramos G (1996) J Pharm Biomed Anal 14:1037
20. Bazylak G, Nagels LJ (2002) J Chromatogr A 973:85
21. Sun XX, Aboul-Enein H-Y (1999) Anal Lett 32:1143
22. van Stefan Staden R-I, Lal B (2006) Anal Lett 39:1311
23. Shen L, Li Z, He P (2010) Electrochem Commun 12:876
24. Huang H-C, Huang S-Y, Lin C-I, Lee Y-D (2007) Anal Chim Acta 582:137
25. Wu J, Li X-L, Wu X-M, Huan S-Y, Shen G-L, Yu R-Q (2005) Chem Res Chin Univ 21:517
26. Chen Y, Duan J-P, Chen H-Q, Liao W-R, Chen G-N (2004) Fenxi Shiyanshi 23:67

27. Pizzariello A, Stred'ansky M, Stred'anska S, Miertus S (2001) Sens Actuator B Chem B76:286
28. Liu L, Pan H, Du M, Xie W, Wang J (2010) Electrochim Acta 55:724
29. Moane S, Smyth MR, O'Keeffe M (1996) Analyst 121:779
30. Guo R-X, Xu Q, Wang D-Y, Hu X-Y (2008) Microchim Acta 161:265
31. Ludwig R (2005) Microchim Acta 152:1
32. Arena G, Contino A, Gulino FG, Magri A, Sansone F, Sciotto D, Ungaro R (1999) Tetrahedron Lett 40:1597
33. Vaze VD, Srivastava AK (2008) J Pharm Biomed Anal 47:177
34. Vaze VD, Srivastava AK (2007) Electrochim Acta 53:1713
35. Valentini F, Amine A, Orlanducci, Terranova ML, Palleschi G (2003) Anal Chem 75:5413
36. Bard AJ, Faulkner LR (1980) Electrochemical methods: fundamentals and applications, 2nd edn. Wiley, New York, p 236
37. Bard AJ, Faulkner LR (1980) Electrochemical methods: fundamentals and applications. Wiley, New York, p 231
38. Xu Q, Wang S-F (2005) Microchim Acta 151:47